# Inclusions in Fluctuating Membranes: Exact Results

Roland R. Netz

J. Phys. I France 7 (1997) 833–852 JULY 1997, PAGE 833

# Inclusions in Fluctuating Membranes: Exact Results

Roland R. Netz (*)

Service de Physique Théorique, CEA-Saclay, 91191 Gif sur Yvette, France

*(Received 13 March 1997, received in final form 24 March 1997, accepted 25 March 1997)*

PACS.82.70.-y – Disperse systems
PACS.87.22.Bt – Membrane and subcellular physics and structure
PACS.64.60.-i – General studies of phase transitions

**Abstract.** — Point-like inclusions in fluid, fluctuating membranes are considered. Here the term inclusion is used in a general sense and describes a number of seemingly disparate situations: particles in membranes or other external and localized forces (such as a laser tweezer) which i) make the membrane locally stiffer, ii) induce a local spontaneous curvature, iii) change the local membrane thickness, or iv) the local separation between neighboring membranes. All these situations can be described by linear or quadratic local perturbations, for which the partition function is calculated exactly using a Gaussian membrane model. The deformed shape of a membrane in response to the presence of one inclusion and the membrane-mediated interactions between inclusions are thus obtained without further approximations. The interaction between two inclusions described by linear perturbations is temperature independent and therefore not affected by membrane fluctuations. The interaction between two inclusions described by quadratic perturbations is solely due to membrane shape fluctuations and vanishes at zero temperatures; in the strong coupling limit it shows a universal logarithmic divergence at short length scales. Formulas for the interaction of $n$ inclusions are derived, which show non-trivial multibody contributions for the case of quadratic inclusions. All these results are valid for all temperatures and for all coupling strengths and thus bridge previously obtained results obtained at zero temperatures (neglecting membrane shape fluctuations) or using perturbation theory (for small strengths of the coupling between the inclusions and the membrane). These exact results are obtained with general Gaussian Hamiltonians and are thus applicable to all systems described by Gaussians forms.

## 1. Introduction

In many experimental situations, membranes incorporate relatively large inclusions (such as proteins) [1–7] or host adsorbed colloidal particles or other macromolecules [8], which locally perturb the elastic and structural properties of the pure membrane [9]. In addition to direct interactions between inclusions, the local membrane perturbations induce spatially decaying responses of the membrane shape and composition, which, often but not necessarily in conjunction with thermally activated fluctuations, lead to rather long-ranged interactions between these inhomogeneities. If the inclusions are free to diffuse laterally, they can as a result organize

(*) *Present address*: Max-Planck-Institut für Kolloid- und Grenzflächenforschung, Kantstr. 55, 14513 Teltow, Germany. (e-mail: netz@mpikg-teltow.mpg.de)

into ordered spatial structures. The experimentally observed behavior for such mixed systems is very complex and shows phase separation of the different membrane constituents, randomly mixed states, and more complicated modes of aggregation of larger inclusions [10–15]. A different and rather new way of experimentally perturbing the local membrane structure and thus to achieve an effect similar to an inclusion is provided by the optical tweezer method; here, characteristic membrane distortion profiles have been observed [16].

The shape deformation of a membrane around an inclusion was theoretically studied using the standard elasticity model of membranes [17], giving rise to attractive or repulsive interactions between two inclusions, depending on the elastic properties of the two monolayers making up the bilayer [18, 19]. These calculations correspond to the zero-temperature limit, where membrane shape fluctuations are neglected. More recently, it has been realized that thermally activated shape fluctuations of the embedding membrane induce additional interactions between inclusions [20–23]. These calculations were either done perturbatively, valid for high temperatures and in the limit where the inclusions are not too different from the embedding membrane (*i.e.*, in the weak-coupling limit) [20–22], or using an expansion in terms of inverse powers of the distance between the inclusions [20, 23].

In this article, we consider inclusions in fluctuating membranes. The membrane fluctuations are governed by a Gaussian Hamiltonian, the inclusions are defined by local linear and quadratic perturbation fields. We obtain the interaction between two (and for inclusions described by linear perturbation also arbitrarily many) inclusions. We also calculate the membrane profile and the roughness profile around a single inclusion, as is relevant for the profile of the distance between two membranes which are held together by a gap junction [24] or a laser tweezer [16]. These results are exact and thus bridge the previous results obtained either in the zero-temperature limit or the perturbative regime. For inclusions described by *linear perturbations*, we obtain that the effective interactions and the membrane profile do not depend on the temperature, *i.e.*, fluctuations of the membrane shape are irrelevant. In this case, our results therefore agree both with previous calculations performed at zero temperatures [19] and perturbation expansions [22]. For inclusions described by *quadratic perturbations* we find the effects to be solely due to membrane shape fluctuations and thus to vanish at zero temperature. In this case, there are non-trivial multi-body interaction terms, which are obtained to leading order in a perturbative analysis. For the interaction between two such inclusions, our exact result shows in the strong-coupling limit a logarithmic divergence for separations smaller than the in-plane membrane correlation length. Due to its logarithmic nature, this divergence had been missed both in perturbation theory [20, 22] and in calculations using an expansion in inverse powers of the distance [20]. Combining a scaling argument with these exact results, we derive the separation profile between two *impenetrable membranes* which are held together at one point. The resulting separation profile increases linearly with the distance from the junction point and thus agrees with previous calculations based on an effective free energy expression [25].

Although not discussed in this article, further possible applications of the exact results derived in Appendix A include inhomogeneous near-critical media and disordered electronic systems.

## 2. Fluctuating Membrane with Inclusions

The effective Hamiltonian of a homogeneous membrane which is on average flat can be written as [26]

$$\mathcal{H}_0 = \int \mathrm{d}^2\mathbf{x} \left\{ \frac{\kappa_0}{2} \left[\nabla^2 l(\mathbf{x})\right]^2 + V[l(\mathbf{x})] \right\}, \tag{1}$$

where $\kappa_0$ is the bending-rigidity modulus of the membrane. This model is applicable to very different situations; accordingly, the displacement field $l(\mathbf{x})$ then describes

i) the shape of a single membrane, subject to an external potential $V(l)$, which can be due to the interaction with some fixed extended object such as a substrate wall or a liquid interface,

ii) the separation between two membranes [27], interacting *via* the mutual potential $V(l)$,

iii) the thickness of a single membrane, in which case $V(l)$ corresponds to the elastic energy associated with the local membrane thickness, and

iv) the position of a membrane inside a stack, where the potential $V(l)$ takes in an approximate fashion the interaction with the neighboring membranes into account [28].

To make the calculations tractable, we use for $V(l)$ a harmonic potential,

$$V(l) = \frac{m}{2} l^2, \tag{2}$$

which approximates other potentials reasonably well if the fluctuations of the membrane are rather small. For strongly fluctuating membranes the impenetrability between membranes becomes important and leads to long-ranged effective repulsive interactions between them [31]. In this case the harmonic approximation does not describe the situation adequately, but a simple scaling argument can be used to obtain results for this important case as well, see Section 5.

We will now discuss the effect of an inclusion (or any other type of local membrane perturbation) on the elastic properties of a membrane defined by Hamiltonian (1). We distinguish four different perturbations, shown schematically in Figure 1:

a) An inclusion (to the left) or an adsorbed particle (to the right) which is stiffer than the embedding membrane constitutes a locus of increased bending rigidity. The energy term representing such an inclusion located at $\mathbf{x}$ is thus $\sim [\nabla^2 l(\mathbf{x})]^2$ and positive [32].

b) An inclusion can be up-down asymmetric and thus also induce a local spontaneous curvature (to the left); for an adsorbed particle the same effect obtains if the adsorbate is rather spherical than plate-like (to the right). The energy term in both cases would be $\sim \nabla^2 l(\mathbf{x})$.

c) A single membrane which is locally confined by some external force or geometrical constraint (to the left) corresponds to a local change of the harmonic amplitude $m$ in equation (2); the same occurs for a trapped particle between two membranes (to the right), which hinders fluctuation in the separation coordinate geometrically. Experimentally, this can also be achieved by so called gap junctions which locally form a connection between two membranes [25, 35, 36], or be applying a laser tweezer [16]. This perturbation can thus be described by an additional local harmonic potential, *i.e.*, a term $\sim l^2(\mathbf{x})$.

d) Finally, a single membrane which is locally pulled at can be described by a local linear perturbation (to the left). The same linear perturbation acts between the two monolayers making up a membrane when an inclusion locally changes the preferred thickness of the membrane (to the right) [19]. The perturbation term in this case is simply $\sim l(\mathbf{x})$.

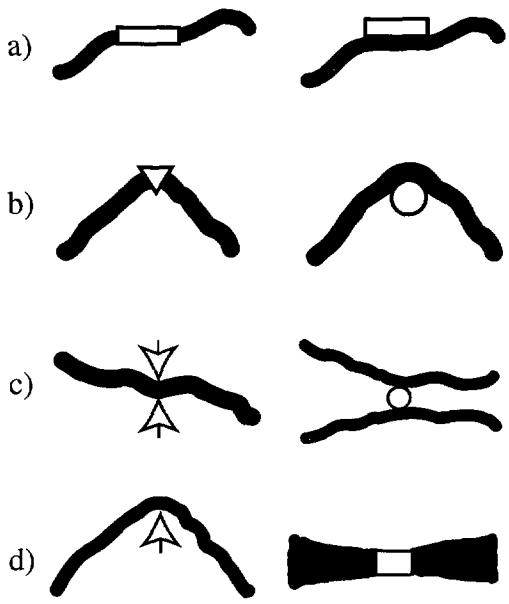


Fig. 1. — Schematic picture of different local membrane perturbations. a) An inclusion or an adsorbed macro particle changing the local bending rigidity, giving rise to a perturbation quadratic in the local curvature ; b) an inclusion or an adsorbed particle giving rise to a local spontaneous curvature; c) an external force or obstacle which confines a single membrane, or a trapped particle or a gap junction between two membranes, giving rise to a strong local confining potential of the membrane height or the separation coordinate, respectively; d) an external force or obstacle which distorts a single membrane, or an inclusion which changes the membrane thickness locally, inducing a perturbation coupling linearly to the membrane coordinate.

In general, one will encounter a mixture of these effects. For example, a gap junction which binds two membranes locally will change both the average separation between the membranes (which is described by a linear perturbation) but also the fluctuations (or the roughness) of this separation coordinate (which is described by a quadratic perturbation). It will be shown for this case, however, that the quadratic perturbation, *i.e.*, the change in the local roughness of the separation coordinate, is more dominant and the linear perturbation can be neglected (see Sect. 5). To make our calculations tractable, we neglect the effect of locally increased Gaussian curvature. We note that the inclusion of such effects leads to interesting and important changes in resulting behavior [20].

Also we only consider point-like inclusions; the perturbation Hamiltonian for $N$ inclusions can then in general be written as

$$\mathcal{H}'_N(\{\mathbf{x}_N\}) = \sum_{i=0}^{N} \left\{ a_i \mathcal{A}(\mathbf{x}_i) + \frac{b_i}{2} \mathcal{A}^2(\mathbf{x}_i) \right\}, \tag{3}$$

which includes linear as well as quadratic perturbations. The linear operator $\mathcal{A}(\mathbf{x})$ occurs in two versions where the local perturbation couples either to the local curvature or the local height variable, *i.e.*,

$$\mathcal{A}(\mathbf{x}) = \begin{cases} l(\mathbf{x}) \\ \triangle l(\mathbf{x}) = \nabla^2 l(\mathbf{x}) \end{cases} \tag{4}$$

and will be denoted by $\mathcal{A}_1$ and $\mathcal{A}_\triangle$ accordingly. With these definitions, one can describe all different situation a)-d) depicted schematically in Figure 1. It is a well established fact that the local perturbation of a membrane due to inclusions induces mutual interactions between them [18–20]. Here, we derive this interaction for all values of the coupling constants, temperature, and in-plane correlation length of the membrane, in which case shape fluctuations have to be taken into account. For $N$ inclusions defined by (3) the free energy $\mathcal{F}_N$ associated with a specific distribution of inclusions is defined as

$$\mathcal{F}_N(\{\mathbf{x}_N\}) = -T \ln \left\{ \frac{\int \mathcal{D}l(\cdot) \mathrm{e}^{-\mathcal{H}_0/T - \mathcal{H}'_N(\{\mathbf{x}_N\})/T}}{\int \mathcal{D}l(\cdot) \mathrm{e}^{-\mathcal{H}_0/T}} \right\} \equiv -T \ln \langle \mathrm{e}^{-\mathcal{H}'_N(\{\mathbf{x}_N\})/T} \rangle_0 \tag{5}$$

and has been calculated perturbatively [20,21] by noting that the first contribution to (5) in an expansion is equivalent to connected correlation functions. The interaction free energy $\Delta\mathcal{F}_N$ is obtained by subtracting the self energy $\mathcal{F}_1$,

$$\Delta\mathcal{F}_N(\{\mathbf{x}_N\}) = \mathcal{F}_N(\{\mathbf{x}_N\}) - N\mathcal{F}_1(\mathbf{x}). \tag{6}$$

We also calculate the shape of the membrane, $\langle l(\mathbf{x}) \rangle$, and the roughness, $\langle l^2(\mathbf{x}) \rangle - \langle l(\mathbf{x}) \rangle^2$, as a function of the distance $\mathbf{x}$ from a single inclusion located at $\mathbf{x} = \mathbf{0}$, which are determined from

$$\langle l(\mathbf{x}) \rangle = \langle l(\mathbf{x}) \mathrm{e}^{-\mathcal{H}'_1(\mathbf{0})/T} \rangle_0, \tag{7}$$

$$\langle l^2(\mathbf{x}) \rangle = \langle l^2(\mathbf{x}) \mathrm{e}^{-\mathcal{H}'_1(\mathbf{0})/T} \rangle_0. \tag{8}$$

## 3. Linear Perturbation

We first consider linear perturbations, *i.e.*, we set $b = 0$ in (3). This applies to the case where the local perturbation breaks the up-down symmetry of the membrane. The result for the free energy of an assembly of $N$ such inclusions with coupling constants $a_i, (i = 1, N)$, is given by (see Appendix A.1)

$$\mathcal{F}_N^{\mathrm{L}}(\{\mathbf{x}_N\}) = -\frac{1}{2T} \sum_{i=1}^{N} \sum_{j=1}^{N} a_i a_j G(\mathbf{x}_i - \mathbf{x}_j) \tag{9}$$

where $G(\mathbf{x}_i - \mathbf{x}_j)$ denotes the correlation function (calculated in Appendix B) defined by

$$G(\mathbf{x}_i - \mathbf{x}_j) \equiv \langle \mathcal{A}(\mathbf{x}_i) \mathcal{A}(\mathbf{x}_j) \rangle_0. \tag{10}$$

3.1. Self Energy. — The self energy $\mathcal{F}_1^{\mathrm{L}}$ can be calculated from the expression for $\mathcal{F}_N^{\mathrm{L}}(\{\mathbf{x}_N\})$ by setting all coupling constants $a_i$ equal to zero except one, which is denoted by $a$; the result is

$$\mathcal{F}_1^{\mathrm{L}} = -a^2 G(0)/2T. \tag{11}$$

Since $G(0)$ is a quadratic expectation value, it is always positive and the linear self energy turns out to be negative; for example a colloid adsorbing on a membrane and inducing a local curvature gains energy due to membrane shape fluctuations [37].

3.2. Interaction Energy. — By subtracting the self energies from the general expression equation (9) one obtains the interaction energy for an assembly of $N$ inclusions, which turns out to be a sum over pair interactions.

$$\Delta\mathcal{F}_N^{\mathrm{L}}(\{\mathbf{x}_N\}) = -\sum_{i=1}^{N} \sum_{j>i}^{N} a_i a_j G(\mathbf{x}_i - \mathbf{x}_j)/T. \tag{12}$$

The correlation function $G$ oscillates with an exponentially damped envelope for arguments larger than the membrane correlation length (see Appendix B). The amplitude of $G$ depends on whether the inclusions couple to the membrane height or the membrane curvature. One finds that inclusions which couple to the membrane height *attract* each other if the coupling constants $a$ have the same sign, and that inclusions which couple to the membrane curvature *repel* each other if the preferred curvature is of the same sign. One also notes that the result (12) agrees exactly with the predictions from a second-order perturbation expansion [22] and that multi-body interaction are absent (there are only quadratic terms in $a_i$ in the expressions (9, 12)). Since the correlation functions $G$ are proportional to the temperature (see Appendix B), it follows that the results for free energies and profiles have no explicit temperature dependence. Therefore fluctuations of the membrane shape are irrelevant and the interactions and profiles at all non-zero temperatures are identical to the results obtained at zero temperatures.

For separations smaller than the correlation length, one obtains for inclusions coupling to the membrane height an *attractive* interaction

$$\Delta\mathcal{F}_2^{\mathrm{L}}(\mathbf{x}_1,\mathbf{x}_2) = -\frac{a_1 a_2}{32\kappa_0}\left(2\xi_{\|}^2 - (\mathbf{x}_1-\mathbf{x}_2)^2\right), \tag{13}$$

and likewise for inclusions coupling to the membrane curvature a *repulsive* interaction

$$\Delta\mathcal{F}_2^{\mathrm{L}}(\mathbf{x}_1,\mathbf{x}_2) = \frac{a_1 a_2}{8\kappa_0\xi_{\|}^2}\left(2\xi_{\|}^2 - (\mathbf{x}_1-\mathbf{x}_2)^2\right). \tag{14}$$

For small separations, the interactions are harmonic.

3.3. Profile and Roughness. — The membrane profile is, according to (7), given by

$$\langle l(\mathbf{x})\rangle_{\mathrm{L}} = \langle l(\mathbf{x})\mathrm{e}^{-a\mathcal{A}(0)/T}\rangle_0. \tag{15}$$

It can be obtained from the two-particle free energy $\mathcal{F}_2^{\mathrm{L}}(\mathbf{x}_1,\mathbf{x}_2)$ by taking a derivative with respect to the coupling constant $a_1$, *i.e.*,

$$\langle l(\mathbf{x}_1-\mathbf{x}_2)\rangle_{\mathrm{L}} = \left.\frac{\partial\mathcal{F}_2^{\mathrm{L}}(\mathbf{x}_1,\mathbf{x}_2)}{\partial a_1}\right|_{a_1=0} \tag{16}$$

The result is

$$\langle l(\mathbf{x})\rangle_{\mathrm{L}} = -aG(\mathbf{x})/T. \tag{17}$$

The roughness can be obtained by taking a further derivative with respect to $a_1$, which leads to

$$\langle l^2(\mathbf{x}_1-\mathbf{x}_2)\rangle_{\mathrm{L}} - \langle l(\mathbf{x}_1-\mathbf{x}_2)\rangle_{\mathrm{L}}^2 = -\left.\frac{\partial^2\mathcal{F}_2^{\mathrm{L}}(\mathbf{x}_1,\mathbf{x}_2)T}{\partial a_1^2}\right|_{a_1=0} = G(0) \tag{18}$$

and thus equals the roughness of the unperturbed membrane. This means that a linear perturbation has no effect on the local roughness at all.

The profile (17) calculated here applies to a number of different experimental situations; it i) describes the shape of a single membrane around an asymmetric inclusion, ii) the shape of the two monolayer making up a bilayer in response to a thickness mismatch around the inclusion, iii) the shape of a membrane on which one pulls locally using an adsorbed magnetic bead in a magnetic field, some other adsorbed colloidal particle in an optical trap, or a tether, and iv) it describes the separation between two membranes which are bound at one point by a gap junction or a laser tweezer *if and only if one neglects the impenetrability of the two membranes.*

For the last example, the profile has been calculated theoretically neglecting membrane shape fluctuations [25]. Using the form of $G(x)$, equation (B.4), our result (17) is identical to the one found in [25]. This confirms our prediction made in the last section that membrane shape fluctuations can be neglected for situations described by linear perturbations. We stress that the result (17) does not take the hard-wall interaction into account, which is important for two impenetrable membranes which are pinned together. This case is treated in Section 5 on a scaling level, leading to a different resulting profile.

For separations larger than the correlation length, the correlation function $G(x)$ is oscillatory with an exponentially decaying envelope. For lateral distances from the binding point much smaller than the correlation length we can use the asymptotic expansion (B.9) and obtain the universal parabolic profile

$$\langle l(\mathbf{x})\rangle_{\mathrm{L}} \simeq \frac{ax^2}{32\kappa_0} \tag{19}$$

Since for a free membrane the correlation length is set by the system size, the above results holds for the whole membrane in this case (if one neglects edge effects).

## 4. Quadratic Perturbations

This type of perturbation is realized for all local fields or inclusions which do not break the up-down symmetry of the membrane. The free energy of two quadratic inclusion is according to (5) defined by

$$\mathcal{F}_2^{\mathrm{Q}}(\mathbf{x}_1,\mathbf{x}_2) = -T\ln\langle \mathrm{e}^{-b_1\mathcal{A}^2(\mathbf{x}_1)/2T - b_2\mathcal{A}^2(\mathbf{x}_2)/2T}\rangle_0. \tag{20}$$

The result is derived in Appendix A.2 and reads

$$\mathcal{F}_2^{\mathrm{Q}}(\mathbf{x}_1,\mathbf{x}_2) = \frac{T}{2}\ln\left[\left(1+\frac{b_1G(0)}{T}\right)\left(1+\frac{b_2G(0)}{T}\right) - \frac{b_1b_2}{T^2}G^2(\mathbf{x}_1-\mathbf{x}_2)\right]. \tag{21}$$

4.1. Self Energy. — The self energy $\mathcal{F}_1^{\mathrm{Q}}$ can be obtained from the expression (21) by setting one of the coupling constants to zero,

$$\mathcal{F}_1^{\mathrm{Q}} = \frac{T}{2}\ln\left(1+\frac{bG(0)}{T}\right). \tag{22}$$

One sees that the self energy is positive and actually diverges logarithmically as the coupling constant $b$ becomes large. This result agrees with the first term of a perturbation expansion, which of course missed the logarithmic divergence [22]. The membrane fluctuations therefore give a contribution to the free energy of adsorption or incorporation of a stiff particle which is unfavorable and the strength of which depends both on the coupling constant $b$ and the membrane roughness $G(0)$.

4.2. Interaction Energy. — The biquadratic interaction energy, after subtraction of the self energy, is given by

$$\Delta\mathcal{F}_2^{\mathrm{Q}}(\mathbf{x}_1,\mathbf{x}_2) = \frac{T}{2}\ln\left[1-\frac{b_1b_2G^2(\mathbf{x}_1-\mathbf{x}_2)}{(T+b_1G(0))(T+b_2G(0))}\right]. \tag{23}$$

This equation is one of our main results and deserves further discussion. First of all, it is important to note that the biquadratic interaction is a pure fluctuation effect which vanishes in the zero-temperature limit; this follows from the fact that the correlation function $G$ is

proportional to $T$ itself (see Appendix B). This stands in contrast to the interaction for linear inclusions, equation (12), which was found to be independent of the temperature. It also follows that for finite coupling constants $b_1$ and $b_2$ the interaction remains finite even for vanishing distance. This is different in the strong-coupling limit, *i.e.*, as $b \to \infty$. This limit is experimentally easily reachable and corresponds to very stiff inclusions or to the strong-binding limit for gap junctions. In that limit we obtain

$$\Delta\mathcal{F}_2^{\mathrm{Q}}(\mathbf{x}_1,\mathbf{x}_2) \simeq \frac{T}{2}\ln\left[1-\frac{G^2(\mathbf{x}_1-\mathbf{x}_2)}{G(0)^2}\right], \tag{24}$$

which now exhibits a universal logarithmic divergence for vanishing separation, regardless of the precise behavior of the correlation function. For very large separations, the correlation function becomes zero and the interaction vanishes. It is interesting to note that this logarithmic divergence at small separations only appears in the strong-coupling limit ($b \to \infty$) and thus has been missed in previous perturbative calculations, where either the coupling constant has been treated as a perturbation parameter [20, 22] or an expansion has been undertaken in the inverse inclusion separation [20, 23]. For separations much smaller than the correlation length (which for a free membrane corresponds to separations smaller than the system size and thus applies to all values of the separation, neglecting edge effects) we obtain with the expansion (B.9)

$$\Delta\mathcal{F}_2^{Q}(\mathbf{x}_1,\mathbf{x}_2) = T\ln(|\mathbf{x}_1-\mathbf{x}_2|/\xi_{\|}). \tag{25}$$

For a free membrane of linear size $L$ one has approximately $\xi_{\|} \approx L$ and therefore the strength of the logarithmic attraction in this case only depends on $L$ and is still of the order of the thermal energy for two inclusions which are separated by $L/e$.

4.3. Multibody Interactions. — Likewise, the interaction for an assembly of three quadratic interactions is

$$\begin{aligned}\Delta\mathcal{F}_3^{\mathrm{Q}}(\mathbf{x}_1,\mathbf{x}_2,\mathbf{x}_3) = \frac{T}{2}\ln\Bigg[1 &- \frac{b_1b_2G^2(\mathbf{x}_1-\mathbf{x}_2)}{(T+b_1G(0))(T+b_2G(0))} - \frac{b_2b_3G^2(\mathbf{x}_2-\mathbf{x}_3)}{(T+b_2G(0))(T+b_3G(0))}\\ &- \frac{b_3b_1G^2(\mathbf{x}_3-\mathbf{x}_1)}{(T+b_3G(0))(T+b_1G(0))} + \frac{2b_1b_2b_3G(\mathbf{x}_1-\mathbf{x}_2)G(\mathbf{x}_2-\mathbf{x}_3)G(\mathbf{x}_1-\mathbf{x}_3)}{(T+b_1G(0))(T+b_2G(0))(T+b_3G(0))}\Bigg],\end{aligned} \tag{26}$$

which has been derived by a resummation of an explicit perturbation expansion up to sixth order in the coupling constants $b_i$. By considering the most singular diagrams of the $n$-multibody interaction, shown in Figure 2, we can generalize the results obtained for two and three inclusions to the case of $N$ inclusions including all multi-body interactions; the proposed interaction energy for $N$ inclusions is

$$\begin{aligned}\Delta\mathcal{F}_N^{\mathrm{Q}}(\{\mathbf{x}_N\}) = \frac{T}{2}\ln\Bigg[1 &- \sum_{n=2}^{N}\frac{(-1)^n}{n}\sum_{i_1\neq\cdots\neq i_n}^{N}\frac{b_{i_1}G(\mathbf{x}_{i_1}-\mathbf{x}_{i_2})}{T+b_{i_1}G(0)}\cdot\cdots\cdot\frac{b_{i_{n-1}}G(\mathbf{x}_{i_{n-1}}-\mathbf{x}_{i_n})}{T+b_{i_{n-1}}G(0)}\\ &\times\frac{b_{i_n}G(\mathbf{x}_{i_n}-\mathbf{x}_{i_1})}{T+b_{i_n}G(0)}\Bigg].\end{aligned} \tag{27}$$

The first sum is over all $n$-body interactions, and the second sum is over all combinations of $n$ out of $N$ inclusions. This expression also fulfills the obvious symmetry relation

$$\begin{aligned}\Delta\mathcal{F}_N^{\mathrm{Q}}(\{\mathbf{x}_N\}, b_N = b'+b'') = {}& \Delta\mathcal{F}_{N+1}^{\mathrm{Q}}(\{\mathbf{x}_N,\mathbf{x}_{N+1}=\mathbf{x}_N\}, b_N=b', b_{N+1}=b'')\\ &+\mathcal{F}_1^{\mathrm{Q}}(\mathbf{x}_N,b')+\mathcal{F}_1^{\mathrm{Q}}(\mathbf{x}_N,b'')-\mathcal{F}_1^{\mathrm{Q}}(\mathbf{x}_N,b'+b''),\end{aligned}$$

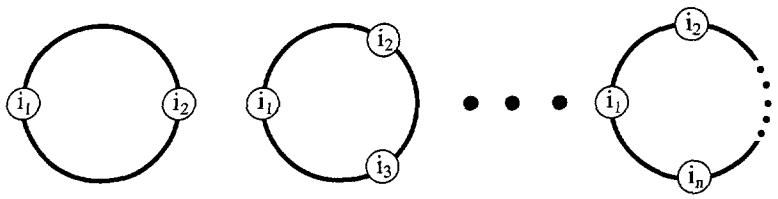


Fig. 2. — Leading two-body, three-body, and $n$-body diagrams for the case of quadratic inclusions. The main index $i$ enumerates the $N$ inclusions, the subindex is used to form subgroups of $n$ inclusions for the $n$-body interactions and to ensure permutation symmetry.

*i.e.*, the interaction between $N$ inclusions can be obtained by contracting the position of any two inclusions in the interaction energy of $N + 1$ inclusions. The important result is that quadratic inclusions, in contrast to the linear case, give nonvanishing and non-trivial multibody interactions.

4.4. PROFILE AND ROUGHNESS. — The membrane profile is not influenced by the presence of a quadratic inclusion, *i.e.*,

$$\langle l(\mathbf{x})\rangle_{\mathrm{Q}} = 0. \tag{28}$$

This can be seen from the fact that the first moment of a quadratic probability distribution vanishes. The roughness profile can be calculated from the expression (21) by taking one derivative with respect to the coupling strength $b_1$,

$$\langle l^2(\mathbf{x}_1 - \mathbf{x}_2)\rangle_{\mathrm{Q}} = 2\,\frac{\partial \mathcal{F}_2^{\mathrm{Q}}(\mathbf{x}_1, \mathbf{x}_2)}{\partial b_1}\bigg|_{b_1=0} \tag{29}$$

and turns out to be

$$\langle l^2(\mathbf{x})\rangle_{\mathrm{Q}} = G(0) - \frac{bG^2(\mathbf{x})}{T + bG(0)}. \tag{30}$$

For finite coupling strength $b$ the roughness at the origin remains finite; for infinite coupling $b = \infty$ one obtains

$$\langle l^2(\mathbf{x})\rangle_{\mathrm{Q}} = G(0) - \frac{G^2(\mathbf{x})}{G(0)} \tag{31}$$

and the roughness at the origin now vanishes. In the limit of free membranes one obtains with the result (B.9)

$$\langle l^2(\mathbf{x})\rangle_{\mathrm{Q}} \simeq G(0)x^2/\xi_{\parallel}^2 \simeq \frac{Tx^2}{16\kappa_0} \tag{32}$$

For the roughness $\xi_{\perp}^{\mathrm{Q}}$ we thus obtain

$$\xi_{\perp}^{\mathrm{Q}}(\mathbf{x}) \equiv \sqrt{\langle l(\mathbf{x})^2\rangle - \langle l(\mathbf{x})\rangle^2} = \sqrt{\frac{T}{\kappa_0}}\frac{|\mathbf{x}|}{4} \tag{33}$$

The width, or the roughness, of the fluctuating membrane thus increases linearly around the pinning site, *i.e.*, the point at which the fluctuations are suppressed.

## 5. Scaling Theory for Impenetrable Membranes

In this section we will be interested in the shape profile of one membrane which is pinned to an impenetrable wall at one point or (which is identical) two impenetrable membrane which are joined at one point. The impenetrability of the membranes lead, due to the concomitant loss of configurational entropy, to a rather long-ranged repulsion between fluctuating membranes, the so-called Helfrich repulsion [31]. This problem has been considered using an effective free energy expression which includes an explicit Helfrich-interaction term and thus takes the fluctuation-induced membrane repulsion in a phenomenological way into account. Two situations have been studied: i) Asymptotically *free* membranes, in which case one obtains a linear, cone-like separation profile around the pinning site [25], and ii) membranes which are *bound* by an additional mutual attraction, in which case one obtains a cone-like profile close to the junction point plus a characteristic overshoot in the separation profile further away from the binding site [38]. In the following, we will be only concerned with the asymptotically free case.

In principle, the impenetrability can be taken into account by adding the hard-wall interaction to the potential $V(l)$ used in equation (1), which however renders the resulting theory intractable. We therefore resort to a scaling ansatz, which uses our exact results from the last sections; this ansatz also leads to a linear separation profile. In order to check the validity of this scaling ansatz (and of the result obtained in [25]), we also consider the case of a polymer pinned to a reflecting wall, a problem which can be solved exactly using path-integral methods (see Appendix C). The exact solution for the polymer case agrees with the corresponding scaling prediction and the result employing a free energy expression similar to the one used in [25], and thus confirms our and Bruinsma et al.'s result for the case of impenetrable membranes.

Let us present the scaling ansatz: For two impenetrable membranes which do not interact *via* some additional long-ranged interaction one expects the general scaling relation [39]

$$\xi_\perp(\mathbf{x}) \sim \langle l(\mathbf{x})\rangle \tag{34}$$

to hold, *i.e.*, the roughness $\xi_\perp$ should locally equal the mean separation $\langle l\rangle$. This is so because in the absence of long-ranged repulsions, the membranes undergo frequent collisions. A gap junction which binds two membranes locally both changes the local separation and the local roughness of the separation coordinate, it therefore can be expressed as a sum of a linear and quadratic local perturbation. First considering the effects of the two types of perturbations separately (and in the absence of the hard-wall interaction), we obtain a quadratic profile for the separation due to the linear perturbation, equation (19), and a linear profile for the roughness due to the quadratic perturbation, equation (33). One sees that the scaling relation (34) is violated: For small distances from the inclusion the roughness is larger than the separation. Let us now consider the hard-wall interaction. It will in general have two effects: it will decrease the roughness and/or increase the membrane separation, such that the scaling relation (34) be satisfied. By comparing the linear and quadratic profiles we find the linear profile to be dominant for distances smaller than a certain crossover length. By matching the separation and the roughness at the boundary of the membrane, we find this crossover length to coincide with the system size. This indicates that the separation profile will differ from (19) and be in fact linear on all length scales,

$$\langle l(\mathbf{x})\rangle \sim \xi_\perp \sim \sqrt{\frac{T}{\kappa_0}}|\mathbf{x}|. \tag{35}$$

Thus we obtain two different predictions for the membrane profile: i) in the case of one localized perturbation pulling on a single membrane or for a gap junction between two membranes in the absence of impenetrability or shape fluctuations, one obtains a quadratic profile,

equation (19), and ii) for a gap junction or a binding site in the case where the membranes are impenetrable and flexible one obtains a linear membrane profile, equation (35). The membrane impenetrability in conjunction with thermally activated shape fluctuations, incorporated in an approximate fashion by using the scaling relation (34), leads to a much more singular separation profile close to the pinning site, due to the Helfrich repulsion exerted on the membranes.

This result is in full accord with the calculations by Bruinsma *et al.* based on the effective free energy expression [25]

$$\mathcal{F} = \int \mathrm{d}^2\mathbf{x} \left\{ \frac{\kappa_0}{2} \left[\nabla^2 l(\mathbf{x})\right]^2 + \frac{c_{\mathrm{fl}} T^2}{2\kappa_0 l^2(\mathbf{x})} \right\}. \tag{36}$$

This expression contains the Helfrich repulsion explicitly and thus takes the membrane impenetrability into account in a phenomenological fashion. The fluctuation-induced repulsion is seen to be rather long-ranged and diverges strongly at short distances. The prefactor $c_{\mathrm{fl}}$ is a universal amplitude and has the numerically determined value $c_{\mathrm{fl}} \approx 0.116$ [29]. The Euler equation resulting from this expression by minimizing with respect to the membrane profile reads

$$\nabla^4 l(\mathbf{x}) - \frac{c_{\mathrm{fl}} T^2}{\kappa_0^2 l^3(\mathbf{x})} = 0. \tag{37}$$

The solution for the profile including the boundary condition at the pinning site, $l(\mathbf{0}) = 0$, is [25]

$$l(\mathbf{x}) \simeq c_{\mathrm{fl}}^{1/4} \sqrt{\frac{T}{\kappa_0}} |\mathbf{x}| \tag{38}$$

and thus agrees with our scaling solution (35). Whereas our scaling solution can be criticized because of the rather uncontrolled use of the scaling relation (34), the solution (38) which is obtained from the free energy expression (36) relies on the validity of the expression used for the Helfrich interaction in spatially inhomogeneous situations. In principle, the Helfrich interaction to be used in (36) will have an $\mathbf{x}$-dependent coefficient.

To verify the results for the membrane profile, equations (35, 38), we performed calculations for the analogous system of a directed polymer, where the difference between the two situations, pinning the polymer to a wall in the presence or absence of impenetrability and shape fluctuations, is obtained exactly using path-integral methods (Appendix C). In the absence of the hard-wall interaction, or at zero temperatures, the average polymer path is linear, see equation (C.3). For a polymer pinned to a hard wall and in the presence of path fluctuations, one obtains a square root dependence of the average polymer path on the distance from the pinning site, see equation (C.18), in agreement with the resulting average polymer path obtained from applying the general scaling relation (34) to the case of polymers, see equation (C.5). The average polymer path can also be calculated using the method of Bruinsma *et al.* The effective free energy expression for polymers analogous to the one for membranes reads

$$\mathcal{F}_{\mathrm{P}} = \int \mathrm{d}x \left\{ \frac{\kappa_0}{2} \left[\nabla l_{\mathrm{P}}(x)\right]^2 + \frac{c_{\mathrm{P}} T^2}{2\kappa_0 l_{\mathrm{P}}^2(x)} \right\}. \tag{39}$$

The Helfrich repulsion for the case of polymers has the same functional form as for membranes with a coefficient which can be calculated exactly (see *e.g.* [40]). The Euler equation for this expression reads

$$\nabla^2 l_{\mathrm{P}}(x) + \frac{c_{\mathrm{P}} T^2}{\kappa_0^2 l_{\mathrm{P}}^3(x)} = 0. \tag{40}$$

The solution for the boundary condition at the pinning site, $l_P(0) = 0$, is

$$l_P(x) \simeq c_P^{1/4} \sqrt{\frac{Tx}{\kappa_0}} \tag{41}$$

and thus agrees both with the corresponding scaling solution (C.5) and with the exact result (C.18). This confirms the result for the membrane profile for two impenetrable fluctuating membranes, equation (35) or (38), and demonstrates the validity of both the effective free energy expression (36) used by Bruinsma *et al.* and the scaling ansatz leading to (35).

## 6. Discussion

The partition functions for systems governed by Gaussian Hamiltonians including linear and quadratic local perturbations are considered. Exact expressions for an arbitrary number of linear and for two quadratic local perturbations are derived. The formulas for quadratic perturbations are generalized to an arbitrary number of inclusions by using a diagrammatic perturbation expansion. These results are applied to two-dimensional membranes, for which expressions for the interactions between inclusions and for the membrane profiles near inclusions are derived. For *linear* inclusions, multi-body effects are absent and the calculated interactions and profiles are independent of the temperature and thus insensitive to membrane shape fluctuations. For this case, our results therefore agree with previous calculations performed at zero temperature and neglecting membrane shape fluctuations. For *quadratic* inclusions, in which case fluctuations are important, there are non-trivial multi-body interaction terms. Also, the two-body interaction shows a logarithmic singularity in the strong-coupling limit for short distances. Such a logarithmic two-body interaction has been shown to lead to strongly aggregated states [25], but the present study indicates that multi-body interactions and thus also the detailed inclusion arrangement will play an important role in determining the aggregation state. Using a scaling argument, the distance profile for a membrane pinned to an impenetrable wall at one point (or for a gap junction between two membranes) is found to be linear and thus in agreement with the cone-like profile found by Bruinsma *et al.* [25] using an effective free-energy expression. In contrast, pulling on a single membrane locally (for example by a laser tweezer or by a tether) without the presence of an impenetrable wall is predicted to lead to a much smoother parabolic distortion profile. This prediction is further substantiated by an exact calculation for a directed polymer in $1+1$ dimensions (Appendix C), which yields at an impenetrable wall and in the presence of path fluctuations a square-root-like average path and in the absence of the impenetrable wall a linear path, in agreement with scaling theory and the Bruinsma Ansatz.

## Acknowledgments

I thank R. Menes and T. Weikl for useful discussions. I am most grateful to H. Orland for enjoyable and enlightening discussions and for introducing me into the methods used in Appendix A.

## Appendix A

### Inclusion Free Energies

A.1 LINEAR INCLUSIONS. — We write the Hamiltonian of the unperturbed membrane as a general Gaussian bilinear kernel,

$$\mathcal{H}_0/T = \frac{1}{2}\int \mathrm{d}\mathbf{x} \int \mathrm{d}\mathbf{x}'\; l(\mathbf{x})G^{-1}(\mathbf{x}-\mathbf{x}')l(\mathbf{x}'), \tag{A.1}$$

where $G^{-1}$ is the functional inverse of the correlation function $G$, *i.e.*,

$$\int \mathrm{d}\mathbf{x}\; G^{-1}(\mathbf{x}-\mathbf{x}')G(\mathbf{x}-\mathbf{x}'') = \delta(\mathbf{x}'-\mathbf{x}''). \tag{A.2}$$

All calculations are performed with this general Gaussian measure, and are thus applicable to any Gaussian system. We also note that we do not choose a specific parametrization of the fluctuating field $L(x)$, such that $x$ could be an external, fixed coordinate system (and $L$ an ordinary field), but also an external coordinate system of a fluctuating (hyper)-surface. The perturbation Hamiltonian for $N$ linear inclusions is given by

$$\mathcal{H}'_N(\{\mathbf{x}_N\})/T = \sum_{i=0}^{N} a_i l(\mathbf{x}_i)/T. \tag{A.3}$$

(The proof also works for more general inclusions defined by a local gradient expansion, which would correspond to couplings to the local area and curvature of the membrane.) With the definition

$$\gamma(\mathbf{x}) \equiv \sum_{i=0}^{N} a_i \delta(\mathbf{x}-\mathbf{x}_i)/T \tag{A.4}$$

the partition function can be written as

$$Z = \int \mathcal{D}l(\cdot) \exp\left\{-\frac{1}{2}\int \mathrm{d}\mathbf{x} \int \mathrm{d}\mathbf{x}'\; l(\mathbf{x})G^{-1}(\mathbf{x}-\mathbf{x}')l(\mathbf{x}') + \int \mathrm{d}\mathbf{x}\; \gamma(\mathbf{x})l(\mathbf{x})\right\}, \tag{A.5}$$

which, using the well-known properties of Gaussian integrals, can be transformed into

$$Z = \int \mathcal{D}l(\cdot) \exp\left\{-\frac{1}{2}\int \mathrm{d}\mathbf{x} \int \mathrm{d}\mathbf{x}'\; \left[l(\mathbf{x})G^{-1}(\mathbf{x}-\mathbf{x}')l(\mathbf{x}') - \gamma(\mathbf{x})G(\mathbf{x}-\mathbf{x}')\gamma(\mathbf{x}')\right]\right\}. \tag{A.6}$$

Dividing by the partition function of the unperturbed membrane system

$$Z_0 = \int \mathcal{D}l(\cdot) \exp\left\{-\frac{1}{2}\int \mathrm{d}\mathbf{x} \int \mathrm{d}\mathbf{x}'\; l(\mathbf{x})G^{-1}(\mathbf{x}-\mathbf{x}')l(\mathbf{x}')\right\} \tag{A.7}$$

the inclusion free energy turns out to be

$$\begin{aligned} \mathcal{F}_N^{\mathrm{L}} &= -T\ln(Z/Z_0) \\ &= -\frac{T}{2}\int \mathrm{d}\mathbf{x} \int \mathrm{d}\mathbf{x}'\; \gamma(\mathbf{x})G(\mathbf{x}-\mathbf{x}')\gamma(\mathbf{x}') \\ &= -\frac{1}{2T}\sum_{i=1}^{N}\sum_{j=1}^{N} a_i a_j G(\mathbf{x}_i-\mathbf{x}_j) \end{aligned} \tag{A.8}$$

which is the result used in Section 3.

A.2 QUADRATIC INCLUSIONS. — We perform the calculation for two inclusions with different coupling constants $b_1$ and $b_2$, located at the positions $\mathbf{y}_1$ and $\mathbf{y}_2$, respectively. Using the definition

$$\gamma(\mathbf{x}) \equiv b_1\delta(\mathbf{x}-\mathbf{y}_1)/T + b_2\delta(\mathbf{x}-\mathbf{y}_2)/T \tag{A.9}$$

the partition function is given by

$$Z = \int \mathcal{D}l(\cdot) \exp\left\{-\frac{1}{2}\int \mathrm{d}\mathbf{x}\int \mathrm{d}\mathbf{x}'\left[l(\mathbf{x})G^{-1}(\mathbf{x}-\mathbf{x}')l(\mathbf{x}') + \delta(\mathbf{x}-\mathbf{x}')\gamma(\mathbf{x})l(\mathbf{x})l(\mathbf{x}')\right]\right\}. \tag{A.10}$$

The result of this Gaussian integral is (up to an unimportant normalization factor which only contributes a constant to the free energy)

$$Z = \left(\ \mathrm{Det}\left[G^{-1}(\mathbf{x}-\mathbf{x}') + \delta(\mathbf{x}-\mathbf{x}')\gamma(\mathbf{x})\right]\right)^{-1/2} \tag{A.11}$$

Again dividing by the unperturbed partition function $Z_0$ as was done in equation (A.8), we obtain the free energy of the inclusions as

$$\mathcal{F}_2^{\mathrm{Q}} = \frac{T}{2}\ \mathrm{Tr}\ \ln\left[\delta(\mathbf{x}-\mathbf{x}') + G(\mathbf{x}-\mathbf{x}')\gamma(\mathbf{x})\right]. \tag{A.12}$$

Expanding the logarithm we can rewrite the expression as

$$\mathcal{F}_2^{\mathrm{Q}} = \frac{T}{2}\sum_{n=1}^{\infty}\frac{(-1)^{n+1}}{n}W_n \tag{A.13}$$

with $W_n$ being defined as

$$W_n \equiv \int \mathrm{d}\mathbf{x}_1 \cdot\quad \mathrm{d}\mathbf{x}_n G(\mathbf{x}_1-\mathbf{x}_2)\gamma(\mathbf{x}_1)G(\mathbf{x}_2-\mathbf{x}_3)\gamma(\mathbf{x}_2)\cdot\quad G(\mathbf{x}_n-\mathbf{x}_1)\gamma(\mathbf{x}_n). \tag{A.14}$$

Introducing the fourier transformed correlation functions we arrive at

$$W_n = \left[\prod_{k=1}^{n}\int \mathrm{d}\mathbf{x}_k\gamma(\mathbf{x}_k)\int \mathrm{d}\mathbf{q}_k\tilde{G}(\mathbf{q}_k)\right]\prod_{k=1}^{n}\mathrm{e}^{\imath\mathbf{q}_k\cdot(\mathbf{x}_k-\mathbf{x}_{k+1})}, \tag{A.15}$$

which by regrouping can be rewritten as

$$W_n = \left[\prod_{k=1}^{n}\int \mathrm{d}\mathbf{x}_k\gamma(\mathbf{x}_k)\int \mathrm{d}\mathbf{q}_k\tilde{G}(\mathbf{q}_k)\right]\prod_{k=1}^{n}\mathrm{e}^{\imath\mathbf{x}_k\cdot(\mathbf{q}_k-\mathbf{q}_{k-1})} \tag{A.16}$$

In these expressions, all variables indexed by $k$ are cyclic variables, *i.e.*, one has $\mathbf{x}_{n+1} = \mathbf{x}_1$ and $\mathbf{q}_{n+1} = \mathbf{q}_1$. Now the integrals over $\mathbf{x}_k$ can be performed, leading to

$$W_n = \left[\prod_{k=1}^{n}\int \mathrm{d}\mathbf{q}_k\tilde{G}(\mathbf{q}_k)\right]\prod_{k=1}^{n}\left[\frac{b_1}{T}\mathrm{e}^{\imath\mathbf{y}_1\cdot(\mathbf{q}_k-\mathbf{q}_{k-1})} + \frac{b_2}{T}\mathrm{e}^{\imath\mathbf{y}_2\cdot(\mathbf{q}_k-\mathbf{q}_{k-1})}\right]. \tag{A.17}$$

By introducing the Ising variables $\sigma_k = \pm 1$ one obtains

$$W_n = \left[\prod_{k=1}^{n}\sum_{\sigma_k}\int \mathrm{d}\mathbf{q}_k\tilde{G}(\mathbf{q}_k)\right]\prod_{k=1}^{n}h(\sigma_k)\mathrm{e}^{\imath(\mathbf{q}_k-\mathbf{q}_{k-1})\cdot([1+\sigma_k]\mathbf{y}_1/2+[1-\sigma_k]\mathbf{y}_2/2)}, \tag{A.18}$$

which by another regrouping can be written as

$$W_n = \left[\prod_{k=1}^{n}\sum_{\sigma_k}\int \mathrm{d}\mathbf{q}_k \tilde{G}(\mathbf{q}_k)\right]\prod_{k=1}^{n} h(\sigma_k)\mathrm{e}^{\mathrm{i}\mathbf{q}_k\cdot(\mathbf{y}_1-\mathbf{y}_2)(1-\sigma_k\sigma_{k+1})/2} \tag{A.19}$$

The function $h(\sigma_k)$, which plays the role of a magnetic field in the Ising model, is given by

$$h(\sigma_k) \equiv b_1(1+\sigma_k)/2T + b_2(1-\sigma_k)/2T. \tag{A.20}$$

Now the integral over $\mathbf{q}_k$ can be performed, and after symmetrizing the transfer matrix, the expression becomes

$$W_n = \sum_{\{\sigma_k\}}\prod_{k=1}^{n}\sqrt{h(\sigma_k)h(\sigma_{k+1})}\left[\frac{1+\sigma_k\sigma_{k+1}}{2}G(0) + \frac{1-\sigma_k\sigma_{k+1}}{2}G(\mathbf{y}_1-\mathbf{y}_2)\right], \tag{A.21}$$

with periodic boundary conditions implied, *i.e.*, $\sigma_{n+1} = \sigma_1$. This expression corresponds to the partition function of an Ising ring in an external magnetic field, which can be calculated by diagonalizing the transfer-matrix. The result is, by using the definition of $h(\sigma_k)$ in equation (A.20), given by

$$\begin{aligned} W_n \;=\; & \left[\frac{b_1+b_2}{2T}G(0) + \sqrt{\frac{(b_1-b_2)^2}{4T^2}G^2(0) + \frac{b_1b_2}{T^2}G^2(\mathbf{y}_1-\mathbf{y}_2)}\right]^n \\ & + \left[\frac{b_1+b_2}{2T}G(0) - \sqrt{\frac{(b_1-b_2)^2}{4T^2}G^2(0) + \frac{b_1b_2}{T^2}G^2(\mathbf{y}_1-\mathbf{y}_2)}\right]^n \end{aligned} \tag{A.22}$$

Reinserting this into the series expansion of the logarithm in the free energy, (A.13), the final result for $\mathcal{F}_2^{\mathrm{Q}}$ is

$$\mathcal{F}_2^{\mathrm{Q}}(\mathbf{y}_1,\mathbf{y}_2) = \frac{T}{2}\ln\left[\left(1+\frac{b_1G(0)}{T}\right)\left(1+\frac{b_2G(0)}{T}\right) - \frac{b_1b_2G^2(\mathbf{y}_1-\mathbf{y}_2)}{T^2}\right]. \tag{A.23}$$

## Appendix B

### Correlation Functions

The bilinear correlation function for the Hamiltonian defined in (1) is diagonal in Fourier space and given by

$$\langle\tilde{l}(\mathbf{q})\tilde{l}(\mathbf{q}')\rangle = \delta(\mathbf{q}-\mathbf{q}')\tilde{G}(\mathbf{q}), \tag{B.1}$$

where the propagator is defined as

$$\tilde{G}(\mathbf{q}) \equiv \frac{T}{\kappa_0}\frac{1}{\mathbf{q}^4 + 4\xi_{\|}^{-4}}. \tag{B.2}$$

The correlation length

$$\xi_{\|} \equiv (4\kappa_0/m)^{1/4} \tag{B.3}$$

is the true correlation length determining the exponential decay of all correlation functions. By performing inverse Fourier transformations one calculates the following correlation functions

$$G_{11}(\mathbf{x}) = \langle l(\mathbf{0})l(\mathbf{x})\rangle = \int \frac{\mathrm{d}^2\mathbf{q}}{(2\pi)^2} \mathrm{e}^{\mathrm{i}\mathbf{q}\cdot\mathbf{x}} \tilde{G}(\mathbf{q}) = \int \frac{\mathrm{d}q}{2\pi} q \mathcal{J}_0(qx) \tilde{G}(q) = -\frac{T\xi_{\|}^2}{4\pi\kappa_0} \mathrm{kei}(\sqrt{2}x/\xi_{\|}), \tag{B.4}$$

$$G_{1\triangle}(\mathbf{x}) = \langle l(\mathbf{0})\triangle l(\mathbf{x})\rangle = -\langle \nabla l(\mathbf{0})\nabla l(\mathbf{x})\rangle = -\int \frac{\mathrm{d}q}{2\pi} q^3 \mathcal{J}_0(qx)\tilde{G}(q) = -\frac{T}{2\pi\kappa_0} \mathrm{ker}(\sqrt{2}x/\xi_{\|}), \tag{B.5}$$

$$G_{\triangle\triangle}(\mathbf{x}) = \langle \triangle l(\mathbf{0})\triangle l(\mathbf{x})\rangle = \int \frac{\mathrm{d}q}{2\pi} q^5 \mathcal{J}_0(qx)\tilde{G}(q) = \frac{T}{K}\delta(x) + \frac{T}{\pi\kappa_0\xi_{\|}^2} \mathrm{kei}(\sqrt{2}x/\xi_{\|}). \tag{B.6}$$

For large arguments, the Thomson functions kei and ker exhibit oscillatory behavior with an exponentially decaying envelope and are given by [41]

$$\mathrm{ker}(z) \simeq \sqrt{\frac{\pi}{2z}} \mathrm{e}^{-x/\sqrt{2}} \cos(-z/\sqrt{2} - \pi/8), \tag{B.7}$$

$$\mathrm{kei}(z) \simeq \sqrt{\frac{\pi}{2z}} \mathrm{e}^{-x/\sqrt{2}} \sin(-z/\sqrt{2} - \pi/8). \tag{B.8}$$

For vanishing argument $x$, $\mathrm{ker}(x)$ is positive and diverges, whereas $\mathrm{kei}(0) = -\pi/4$. For separations smaller than the in-plane correlation length, $x \ll \xi_{\|}$, the correlation function $G_{11}(\mathbf{x})$ is given by

$$G_{11}(\mathbf{x}) \doteq \frac{T}{\kappa_0}\left(\frac{\xi_{\|}^2}{16} - \frac{x^2}{32}\right) + \mathcal{O}(x^4\xi_{\|}^{-2}). \tag{B.9}$$

For the roughness, given by $G(0)$, one thus obtains

$$G_{11}(0) = \frac{T\xi_{\|}^2}{16\kappa_0} \tag{B.10}$$

The analogous results for $G_{1\triangle}(0)$ and $G_{\triangle\triangle}(0)$ are infinity, which shows that for these correlation functions the upper momentum cutoff becomes important at small distances. The results for a finite upper momentum cutoff $2\pi/c$ and zero separation are

$$G_{1\triangle}(0) = \frac{T}{8\pi\kappa_0} \log\left(1 + 4\pi^4 \frac{\xi_{\|}^4}{c^4}\right), \tag{B.11}$$

$$G_{\triangle\triangle}(0) = \frac{T}{\kappa_0}\left(\frac{\pi}{c^2} - \frac{1}{4\xi_{\|}^2}\right). \tag{B.12}$$

The results obtained with the infinite cut-off, equations (B.5, B.6), are valid for distances larger than the inverse cutoff, *i.e.*, roughly for $x \approx c$.

## Appendix C

### Polymer Profile Near an Impenetrable Wall

For polymers all the results obtained for membranes can be calculated exactly, which allows a valuable test of the scaling predictions for the membrane profiles near inclusions. We note that the results (17) and (30) for the profiles in presence of a linear and quadratic perturbation, respectively, are valid for polymers, also. This follows since the derivation only uses the Gaussian property of the Hamiltonian. The correlation function for polymers is easily calculated: The Hamiltonian of the directed polymer in $1+1$ dimensions can be written as

$$\mathcal{H}_0 = \int \mathrm{d}x \left\{ \frac{\kappa_0}{2} [\nabla l(x)]^2 + V[l(x)] \right\}. \tag{C.1}$$

Employing a harmonic potential of the form (2), the correlation function is obtained as [40]

$$G^{\mathrm{P}}(x) = \frac{T}{2\kappa_0} \xi_{\|} \mathrm{e}^{-x/\xi_{\|}} \tag{C.2}$$

with the correlation length given by $\xi_{\|} = \sqrt{\kappa_0/m}$. In the limit of infinite correlation length, the results for the profiles (obtained from Eqs. (17, 30)) become

$$\langle l(x) \rangle_{\mathrm{L}}^{\mathrm{P}} \simeq \frac{ax}{2\kappa_0}, \tag{C.3}$$

$$\langle l^2(x) \rangle_{\mathrm{Q}}^{\mathrm{P}} \simeq \frac{Tx}{\kappa_0} \tag{C.4}$$

Using the scaling relation $\langle l^2(x) \rangle \sim \langle l(x) \rangle^2$, we obtain for the polymer profile near a pinning site at an impenetrable wall a profile

$$\langle l(x) \rangle_{\mathrm{Q}}^{\mathrm{P}} \simeq \sqrt{\frac{Tx}{\kappa_0}}. \tag{C.5}$$

The presence of the hard wall changes the polymer path profile from a linear one, equation (C.3), to a square-root profile. This prediction is analogous to the one in (35) obtained for membranes. For the present case of polymers, this profile can be calculated exactly within the path-integral formalism. To this end, one introduces the end-point distribution functions for a polymer of length $X$

$$q(l,x) = \int_0^{\infty} \mathcal{D}l(\cdot) \delta[l(x) - l] \exp\left\{ -\frac{1}{T} \int_0^x \frac{\kappa_0}{2} [\nabla l(x')]^2 + V[l(x')] \mathrm{d}x' \right\}, \tag{C.6}$$

$$q^{\dagger}(l,x) = \int_0^{\infty} \mathcal{D}l(\cdot) \delta[l(x) - l] \exp\left\{ -\frac{1}{T} \int_x^X \frac{\kappa_0}{2} [\nabla l(x')]^2 + V[l(x')] \mathrm{d}x' \right\}, \tag{C.7}$$

which satisfy the diffusion equations

$$\frac{\partial q(l,x)}{\partial x} = \frac{T}{2\kappa_0} \frac{\partial^2 q(l,x)}{\partial l^2} - \frac{V(l)}{T} q(l,x), \tag{C.8}$$

$$\frac{-\partial q^{\dagger}(l,x)}{\partial x} = \frac{T}{2\kappa_0} \frac{\partial^2 q^{\dagger}(l,x)}{\partial l^2} - \frac{V(l)}{T} q^{\dagger}(l,x). \tag{C.9}$$

The normalized Green's functions in the case of vanishing potentials for these equations are

$$q(l,x,l_0) = \sqrt{\frac{\kappa_0}{2T\pi x}} \exp\left\{-\frac{\kappa_0(l-l_0)^2}{2Tx}\right\}, \tag{C.10}$$

$$q^\dagger(l,x,l_X) = \sqrt{\frac{\kappa_0}{2T\pi(X-x)}} \exp\left\{-\frac{\kappa_0(l-l_X)^2}{2T(X-x)}\right\}, \tag{C.11}$$

which satisfy the initial conditions $q(l,0,l_0) = \delta(l-l_0)$ and $q^\dagger(l,X,l_X) = \delta(l-l_X)$. The end-point distributions for the case of an impenetrable wall can be obtained using the method of images. For the distribution of the polymer starting at the wall one obtains

$$q(l,x) \sim \lim_{d\to 0} \left(q(l,x,d) - q(l,x,-d)\right) \tag{C.12}$$

which after normalization reads

$$q(l,x) = \frac{\kappa_0 l}{Tx} \exp\left\{-\frac{\kappa_0 l^2}{2Tx}\right\}. \tag{C.13}$$

The end-point distribution starting at the free end is

$$q^\dagger(l,x) \sim \int_0^\infty \mathrm{d}l_X \left(q^\dagger(l,x,l_X) - q^\dagger(l,x,-l_X)\right) \tag{C.14}$$

which after the integration yields

$$q^\dagger(l,x) \propto \operatorname{erfc}\left(\sqrt{\frac{\kappa_0/2T}{X-x}}\, l\right). \tag{C.15}$$

Note that this expression is not normalizable. For small arguments, *i.e.* in the limit of an infinitely long polymer, the error function is linear, and so the normalized probability distribution to find the polymer at position $x$ at height $l$, defined as

$$\mathcal{P}(l,x) = q(l,x)q^\dagger(l,x)Z^{-1} \tag{C.16}$$

where $Z = \int \mathrm{d}l q(l,L)$ is the partition function of the polymer, is given by

$$\mathcal{P}(l,x) = \frac{2}{\sqrt{2\pi}} \left(\frac{\kappa_0}{xT}\right)^{3/2} l^2 \exp\left\{-\frac{\kappa_0 l^2}{2xT}\right\}. \tag{C.17}$$

The average polymer path is thus given by

$$\langle l(x)\rangle \equiv \int_0^\infty \mathrm{d}l \mathcal{P}(l,x)\, l = \sqrt{\frac{8Tx}{\pi\kappa_0}} \tag{C.18}$$

and thus agrees with the scaling prediction (C.5) and the result of a calculation using an effective free energy expression including the phenomenological Helfrich term, see equations (39-41).

## References


[1] Marčelja S., *Biochim. Biophys. Acta* **455** (1976) 1.
[2] Schröder H., *J. Chem. Phys.* **67** (1977) 1617.
[3] Owicki J.C., Springgate M.W. and McConnell H.M., *Proc. Natl. Acad. Sci. USA* **75** (1978) 1616; Owicki J.C. and McConnell H.M., *ibid.* **76** (1979) 4750.
[4] Jähnig F., *Biophys. J.* **36** (1981) 329.
[5] Mouritsen O.G. and Bloom M., *Biophys. J.* **46** (1984) 141.
[6] Fournier J.B., *Phys. Rev. Lett.* **76** (1996) 4436.
[7] Holzlöhner R., to be published.
[8] Lipowsky R., *Europhys. Lett.* **30** (1995) 197; Hiergeist C. and Lipowsky R., *J. Phys. II France* **6** (1996) 1465.
[9] Goulian M., *Current Opinion Coll. & Int. Sci.* **1** (1996) 358.
[10] Sackmann E., Kotulla R. and Heiszler F.-J., *Can. J. Biochem. Cell Biol.* **62** (1984) 778.
[11] Lewis B.A. and Engelman D.M., *J. Mol. Biol.* **166** (1983) 203.
[12] Pearson L.T., Edelman J. and Chan S.I., *Biophys. J.* **45** (1984) 863.
[13] Blankenburg R., Meller P., Ringsdorf H. and Salesse C., *Biochemistry* **28** (1989) 8214.
[14] Sternberg B., Watts A. and Cejka Z., *J. Struct. Biol.* **110** (1993) 196.
[15] Knoll W., *Ber. Bunsenges. Phys. Chem.* **98** (1994) 512.
[16] Bar-Ziv R. and Moses E., *Phys. Rev. Lett.* **73** (1994) 1392; (1994); Bar-Ziv R., Menes R., Moses E. and Safran S.A., *Phys. Rev. Lett.* **75** (1995) 3356.
[17] Helfrich W., *Z. Naturforsch.* **28c** (1973) 693.
[18] Gruler H., *Z. Naturforsch.* **30c** (1975) 608.
[19] Dan N., Pincus P. and Safran S.A., *Langmuir* **9** (1993) 2768; Dan N., Berman A., Pincus P. and Safran S.A., *J. Phys. II France* **4** (1994) 1713.
[20] Goulian M., Bruinsma R. and Pincus P., *Europhys. Lett.* **22** (1993) 145; *ibid.* **23** (1993) 155.
[21] Palmer K.M., Goulian M. and Pincus P., *J. Phys. II France* **4** (1994) 805.
[22] Netz R.R. and Pincus P., *Phys. Rev. E* **52** (1995) 4114.
[23] Golestanian R., Goulian M. and Kardar M., *Europhys. Lett.* **33** (1996) 241.
[24] Lowenstein W.R., *Physiol. Rev.* **61** (1981) 829.
[25] Bruinsma R., Goulian M. and Pincus P., *Biophys. J.* **67** (1994) 746.
[26] For recent reviews, see "Statistical Mechanics of Membranes and Surfaces", D. Nelson, T. Piran and S. Weinberg, Eds. (World Scientific, Singapore, 1989); 'The Structure and Dynamics of Membranes", R. Lipowsky and E. Sackmann, Eds., Handbook on Biological Physics, Vol. 1 (Elsevier, Amsterdam, in press).
[27] For the case of two membranes, the effective rigidity $\kappa_0$ is a function of the bending rigidities of the two individual membranes, $\kappa_1$ and $\kappa_2$, and is given by $\kappa_0 = \kappa_1\kappa_2/(\kappa_1+\kappa_2)$.
[28] The separation coordinates between neighboring membranes in a stack are indeed decoupled to a good approximation if the membranes are bound by a rather long-ranged potential, such as an external pressure [29]. For short-ranged potentials the situation is more complex, but the decoupling Ansatz describes the situation still rather well [30].
[29] Netz R.R. and Lipowsky R., *Europhys. Lett.* **29** (1995) 345.
[30] Netz R.R. and Lipowsky R., *Phys. Rev. Lett.* **71** (1993) 3596.
[31] Helfrich W., *Z. Naturforsch.* **33a** (1978) 305.
[32] Note that holes correspond to membrane perturbations where the local bending rigidity is reduced [33]. The aggregation of such holes into a hexagonal array or the condensation into a macroscopic single hole has recently been demonstrated for a swollen diblock copolymer system [34]. The parameter controlling which behavior dominates is

the spontaneous curvature of a monolayer, which is for diblock copolymer determined by the block asymmetry.
[33] See for example Goos J. and Gompper G., *J. Phys. I France* **3** (1993) 1551.
[34] Netz R.R. and Schick M., *Phys. Rev. E* **53** (1996) 3875.
[35] Zuckermann D. and Bruinsma R., *Phys. Rev. Lett.* **74** (1995) 3900.
[36] Lipowsky R., *Phys. Rev. Lett.* **77** (1996) 1652.
[37] This effect could be detected by measuring the adsorption coefficient of colloidal particles in a stack of membranes.
[38] Menes R. and Safran S.A., to be published.
[39] See for example Lipowsky R., *Nature* **349** (1991) 475.
[40] Netz R.R., *Phys. Rev. E* **51** (1995) 2286.
[41] Handbook of Mathematical Functions, M. Abramowitz and I.A. Stegun Eds. (Dover Publications, New York, 1972); Gradshteyn I.S. and Ryzhik I.M., Table of Integrals, Series, and Products (Academic Press, New York, 1980).